Materials Letters 362 (2024) 136235

Contents lists available at ScienceDirect

Materials Letters

journal homepage: www.elsevier.com/locate/matlet

Local atomic structural behavior in amorphous and crystalline diphosphate glasses co-doped by different transition metal ions (Ni^{2+}, Cu^{2+} and Co^{2+}): XAFS and XRD analysis

Yousf Islem Bourezg [a,*], Mohamed Kharroubi [a], Messaoud Harfouche [b], Foudil Sahnoune [c], Amar Djemli [c], Djamel Bradai [d]

[a] Physico-chemistry of Materials and Environment Laboratory, Ziane Achour University of Djelfa, BP 3117, Algeria
[b] Synchrotron-light for Experimental Science and Applications in the Middle East (SESAME), Allan 19252, Jordan
[c] Physics Department, University of M'sila, 28000, Algeria
[d] Faculty of Physics, University of Sciences and Technology Houari Boumediene, BP 32, El-Alia 16111, Algiers, Algeria

ARTICLE INFO

Keywords:
EXAFS
XRD
Phosphate glass
Transition metals
Order and disorder
$Na_2ZnP_2O_7$

ABSTRACT

In this study, structural features of $Na_2M_xZn_{1-x}P_2O_7$ (M = Cu, Ni and Co; x = 0 and 5 mol %) glass compounds were investigated. X-ray diffraction (XRD) and X-ray Absorption Fine Structure (XAFS) analysis techniques were used to investigate the phase identification and the local atomic environment around Zn element. Non-doped and Cu co-doped compounds show an amorphous glassy character while a tetragonal $Na_2ZnP_2O_7$ phase was observed in Ni or Co co-doped samples. Fourier-transformed magnitudes of the Extend X-ray Absorption Fine Structure (EXAFS) show a disorder state for pure sample and copper doping compound. On the other hand, nickel or cobalt co-doped compounds show a structural order by the formation of ZnP_2O_7 sheet. Therefore, transition metals (TMs) co-doped phosphate glass play a key role in the structural order /disorder of the glass compounds, by maintaining and reinforcing or even weakening the network structure.

1. Introduction

Glass materials have significantly attracted the interest of researchers due to the wide range of their applications. Phosphate-based glasses are the better choice for sodium-ion batteries [1], storage of nuclear waste [2] and other applications. The most known of phosphate-based glasses, diphosphates structures with a general formula $A_2BP_2O_7$, where A is a monovalent cation and B is a divalent ion [3]. The industrial application range of these glasses is expanded by adding TMs. As different TMs ions (like, Cu, Fe, Zn, Ni, Co) can be successfully introduced on the B site, consequently, many properties can be improved [4–6], such as energy storage capacity [4]. Furthermore, these ions are responsible for the depolymerization process in the phosphate glass, causing structural changes in the glass network.

Several studies were focused only on electric, dielectric and structural properties of Zn-P_2O_7 based-glasses [6,7]. However, the structural role of TMs in many oxide glasses is not yet well understood and the incorporation of such elements to the phosphate host significantly alters the structural characteristics and other physical properties. In the author's opinion, up to now, no experimental studies have been devoted to the local atomic environment and crystal structure identification of diphosphate compounds $Na_2M_xZn_{1-x}P_2O_7$ (M=Cu, Ni and Co; x = 0 and 5 mol %) using XAFS and XRD techniques. Therefore, the main goal of the present study is to investigate the local atomic structure around Zn K-edge of these glasses using XAFS and XRD measurements.

2. Experimental

Phosphate glass compounds were prepared with a chemical composition of $Na_2M_xZn_{1-x}P_2O_7$ (M=Cu, Ni and Co; x = 0 and 5 mol %). Four samples were labeled as NZPO (x = 0), NZPO/5Cu, NZPO/5Ni and NZPO/5Co.

Previously published research provides more details on the used powders and the process of preparing the glasses [8].

XRD data were collected on XPERT-Pro diffractometer with monochromatic Cu-K_α radiation, operating at 40 mA and 40 kV with a scan step of 0.02° for crystal structure identification.

XAFS data were collected at room temperature in fluorescence mode

* Corresponding author.
E-mail address: y.bourezg@univ-djelfa.dz (Y. Islem Bourezg).

https://doi.org/10.1016/j.matlet.2024.136235
Received 30 November 2023; Received in revised form 29 January 2024; Accepted 27 February 2024
Available online 29 February 2024

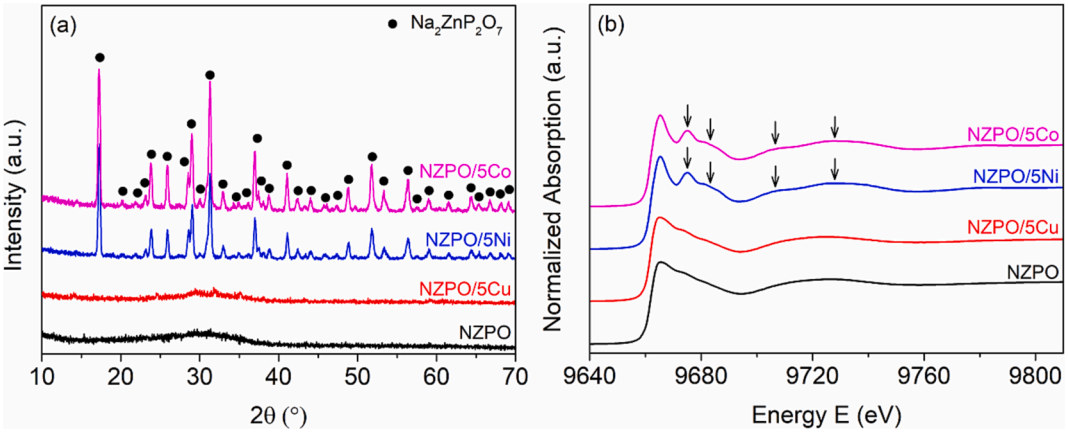

Fig. 1. A) XRD patterns, b) normalized xanes spectra at Zn K-edge.

at the Zn K-edge (9695 eV) on all samples at the BM08-XAFS/XRF beamline, SESAME Synchrotron facility, Jordan [9]. Using Si (1 1 1) double crystal monochromator, XAFS data were recorded in step-by-step mode. Collected XAFS data were processed and analyzed using Demeter software package [10].

3. Results and discussion

3.1. Phase identification using XRD analysis

XRD patterns for the pure and doped samples are shown in Fig. 1a. The diffractograms of non-doped and Cu co-doped NZPO glass samples show an amorphous glassy structure. Therefore, the amorphous state is maintained by adding the Cu element to the NZPO glass. However, Ni or Co substituted into NZPO network leads it to crystallize within the tetragonal structure $Na_2ZnP_2O_7$ (PDF 01-087-0499), as shown in Fig. 1a. This finding is consistent with a previous study [11].

3.2. XAFS data analysis

X-ray absorption near edge structure (XANES) spectra at the Zn K-edge for different samples, are shown in Fig. 1b. The spectra of all compounds show no shift in energy with the presence of a higher peak at 9659 eV which corresponds to the absorption at the Zn K-edge. However, post edge features sensitive to multiple scattering, separating the samples to two categories. As can be seen from Fig. 1b, the NZPO/5Cu sample is identical to the non-doped state, while NZPO/5Ni and NZPO/5Co samples show post edge peaks and oscillations that differ from the other samples, as indicated by the arrows. Therefore, it can be assumed that the TMs have acted as a structural modifier in the present NZPO material.

Fig. 2(a–d) shows the experimental and fitted spectra of k^3-weighted EXAFS oscillation function $k^3\chi(k)$ at the Zn K-edge of the present compounds. Their corresponding magnitudes $\chi(R)$ and real part $Re[\chi(R)]$, are shown in Fig. 2(e–h). The results derived from the fitting are given in Table 1.

From Fig. 2, the NZPO, NZPO/5Cu samples exhibit similar trend in terms of spectra and are different from the samples Ni/Co co-doped NZPO confirming the XANES results in Fig. 1b. The NZPO/5Ni and NZPO/5Co compounds show higher amplitudes in their $k^3\chi(k)$ ($\pm$ 6 $Å^{-3}$) and $\chi(R)$ (10 $Å^{-4}$) spectra than the other samples ($\pm$ 4 $Å^{-3}$ and 7.5 $Å^{-4}$), respectively. Moreover, two new peaks around 5.5 and 8.8 $Å^{-1}$ appeared in Ni/Co doped samples, which belong to the Zn-P and Zn-O shells, as shown in Fig. 2(c and d). On the other hand, high features peaks in $Re[\chi(R)]$ spectra can also be observed for Ni/Co-doped samples up to 3 Å.

The averaged coordination number (N) for both NZPO and NZPO/5Cu samples is 3.4 for oxygen atoms with bond length R of 1.95 Å as the first shell and 2.8 zinc atoms as the second neighbors at 3.21 Å, respectively. Thus, ZnO_4 tetrahedra are formed where the Zn tetrahedron shares almost three vertices with other ZnO_4 units. These findings are consistent with the structural disorder and repeated ZnO_4 tetrahedra of amorphous ZnO-like structure which was confirmed by XRD analysis.

The substitution of nickel and cobalt into NZPO glass favors the formation of $Na_2ZnP_2O_7$ phase by the formation of four shells. The first, third and fourth peaks are linked to Zn-O bands while the second is associated with the Zn-P bonds. The Zn tetrahedral element is surrounded by 3.8 oxygen atoms at a distance 1.91 Å (first shell), 3.5 phosphorus atoms at a distance 3.5 Å, 7 oxygen atoms at a bond length 3.17 Å and 2 oxygen atoms at 3.30 Å. This confirms that the atomic environments of the Ni/Co containing compounds are made up by layers containing ZnO_4 tetrahedral sharing corners with PO_4 units, and therefore forming the ZnP_2O_7 sheet that is the ground of $Na_2ZnP_2O_7$ phase. The increase in neighboring elements almost as natural number in the first shell may be associated with the structural order made by Ni/Co doping atoms. The short-range environment of the present compounds and $Na_2ZnP_2O_7$ crystal structure plots [6,7,11], are presented in Fig. 3(a–c).

It is obvious that the substitution of nickel or cobalt into phosphorus matrix weakens its structure and leads to rapid order via its crystallization during the preparation process. Previously, a lower depolymerization degree was reported in the phosphate network caused by Cu^{2+} ions than the Co^{2+} and Ni^{2+} ones [8], which confirms the structural order in nickel and cobalt doping glass. On the other hand, the activation energy of relaxation (ΔE_τ) decreased as the cobalt amount increased, leading to faster relaxation of the compound matrix [12]. Furthermore, higher values of the activation energy of ion transport (ΔE_{dc}) have been reported for non-doped (91.66 kJ mol^{-1}) and 5 mol % of copper co-doped-NZPO samples (100 kJ mol^{-1}), as compared to 5 mol % (Co or Ni) co-doped-NZPO (85.87 kJ mol^{-1}) glasses [8]. The lowest value of ΔE_{dc} was related to the openness of the network resulting in the weakening of the phosphate structure, as compared to the Cu-doped glass sample which showed the strongest one [8]. Therefore, Cu co-doped NZPO glass might build strong bonds between itself and the surrounding oxygen ions, resulting in an increase of the required energy to break these bonds and thereby delaying its crystallization phenomenon. Hence, a structural disorder is noticed.

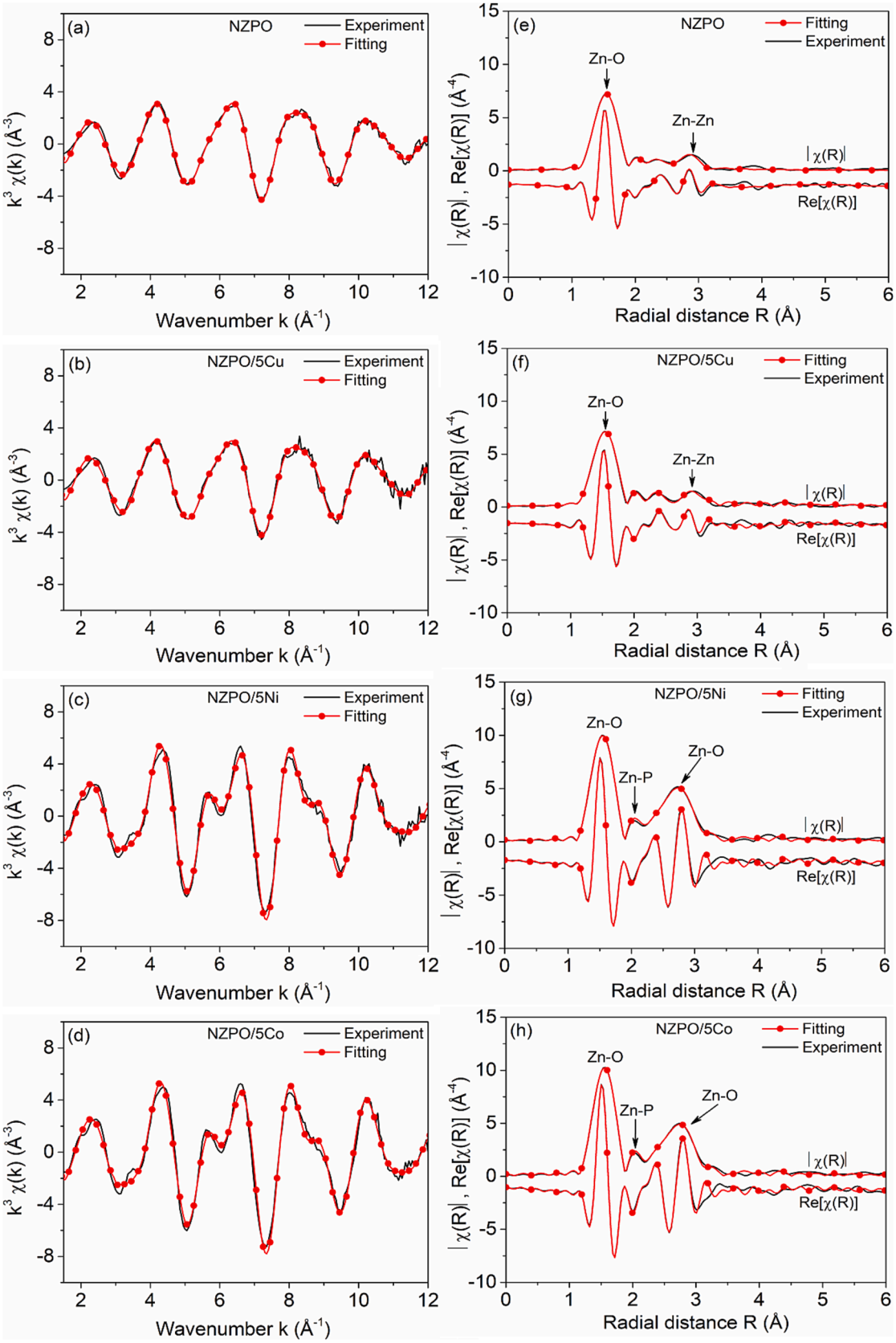

Fig. 2. (a–d): k^3-weighted EXAFS spectral oscillations, (e–h): Fourier transformed EXAFS signals and their real parts.

Table 1
Structural parameters derived from EXAFS fitting; (ΔE is the phase energy, S_0^2 is the amplitude reduction factor and σ^2 is the Debye-Waller factor).

Sample	Shell/Phase	N	R (Å)	σ^2 (Å^2)	ΔE (eV)	S_0^2
NZPO	Zn-O/(ZnO)	3.40	1.95	0.003	3.80	0.89
	Zn-Zn/(ZnO)	2.80	3.21	0.010		
NZPO/5Cu	Zn-O/(ZnO)	3.40	1.95	0.003		
	Zn-Zn/(ZnO)	2.90	3.21	0.010		
NZPO/5Ni	Zn-O/($Na_2ZnP_2O_7$)	3.80	1.91	0.002	3.76	
	Zn-P/($Na_2ZnP_2O_7$)	3.20	2.97	0.008		
	Zn-O/($Na_2ZnP_2O_7$)	5.90	3.17	0.009		
	Zn-O/($Na_2ZnP_2O_7$)	2.10	3.30	0.008		
NZPO/5Co	Zn-O/($Na_2ZnP_2O_7$)	3.90	1.92	0.003	3.80	
	Zn-P/($Na_2ZnP_2O_7$)	3.70	3.00	0.007		
	Zn-O/($Na_2ZnP_2O_7$)	8.00	3.16	0.008		
	Zn-O/($Na_2ZnP_2O_7$)	1.50	3.29	0.008		

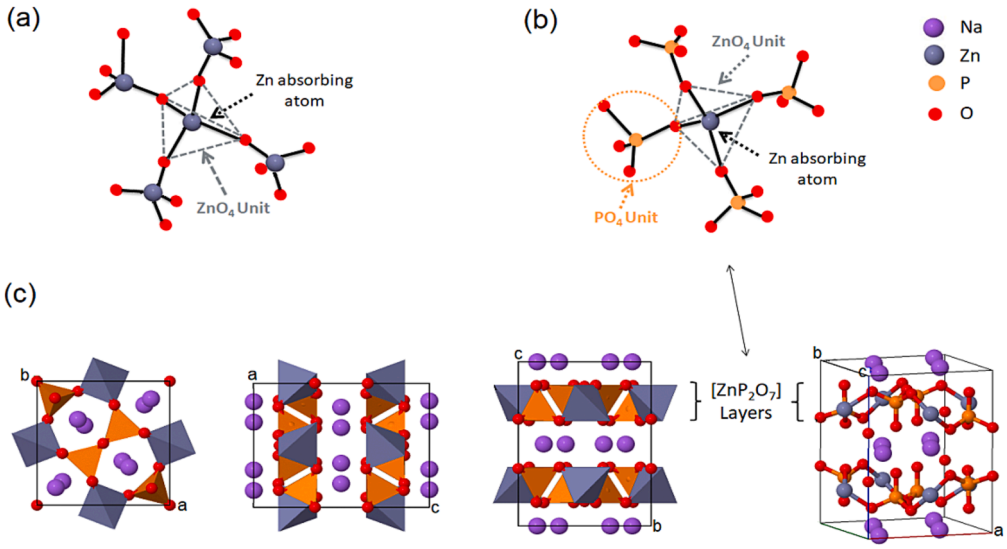

Fig. 3. Short range environment in: a) NZPO and NZPO/5Cu, b) NZPO/5Ni and NZPO/5Co samples, c) $Na_2ZnP_2O_7$ crystal structure plots.

4. Summary and conclusions

The phase identification and local atomic structure around Zn element were investigated in the $Na_2M_xZn_{1-x}P_2O_7$ (M = Cu, Ni and Co; x = 0 and 5 mol %) compounds using XRD and XAFS techniques. Several significant conclusions can be drawn, which are: (i) An amorphous glassy structure is observed in non-doped and copper co-doped NZPO compounds, whereas, nickel or cobalt doped NZPO matrix crystallized forming the $Na_2ZnP_2O_7$ phase. (ii) The EXAFS features are strongly affected by TMs doping compounds. (iii) The repeated ZnO_4 tetrahedra confirm the amorphous ZnO like-nature of the non-doped and Cu co-doped compounds. (iv) Nickel or cobalt substituted into NZPO network show the formation of ZnP_2O_7 sheet, hence, the $Na_2ZnP_2O_7$ phase. (v) TMs play a significant role as structural modifiers, where copper elements maintain and reinforce the amorphous glass disorder, whereas, nickel and cobalt atoms weaken the glass network and lead to its crystallization upon the synthesizing process.

CRediT authorship contribution statement

Yousf Islem Bourezg: Writing – original draft, Formal analysis, Data curation. **Mohamed Kharroubi:** Writing – original draft, Data curation. **Messaoud Harfouche:** Writing – original draft, Investigation. **Foudil Sahnoune:** Investigation. **Amar Djemli:** Investigation. **Djamel Bradai:** Writing – original draft.

Declaration of competing interest

The authors declare that they have no known competing financial interests or personal relationships that could have appeared to influence the work reported in this paper.

Data availability

Data will be made available on request.

Acknowledgements

The authors gratefully acknowledge the support of Synchrotron-light for Experimental Science and Applications in the Middle East, SESAME, for XAFS data collection (Proposal no: 20220137).

References

[1] N. Yubin, Y. Zhang, M. Xu, J. Mater. Chem. A 7 (2019) 15006–15025, https://doi.org/10.1039/C9TA04274A.
[2] J.C. Akhilesh, M. Roy, D.P. Dutta, R.K. Mishra, S.S. Meena, R. Kumar, D. Bhattacharyya, R. Alexander, C.P. Kaushik, A.K. Tyagi, J. Non-Cryst. Solid. 570 (2021) 121016, https://doi.org/10.1016/j.jnoncrysol.2021.121016.
[3] B. Prabeer, J. Lu, T. Ye, M. Kajiyama, S.C. Chung, N. Yabuuchi, S. Komaba, A. Yamada, RSC Adv. 3 (2013) 3857–3860, https://doi.org/10.1039/C3RA23026K.
[4] A.A. Kulkarni, N.K. Gaikwad, A.P. Salunkhe, R.M. Dahotre, T.S. Bhat, J. Electroanal. Chem. 948 (2023) 117795, https://doi.org/10.1016/j.jelechem.2023.117795.

[5] Y. Niu, Y. Zhang, M. Xu, J. Mater. Chem. A 7 (2019) 15006–15025, https://doi.org/10.1039/C9TA04274A.
[6] C. Ferrara, C. Ritter, P. Mustarelli, C. Tealdi, J. Phys. Chem. C 126 (2022) 701–708, https://doi.org/10.1021/acs.jpcc.1c08753.
[7] Y.F. Shepelev, M.A. Petrova, A.S. Novikova, A.E. Lapshin, Glass Phys. Chem. 28 (2002) 317–321, https://doi.org/10.1023/A:1020752811708.
[8] C. Kalai, M. Kharroubi, L. Gacem, S. Balme, A. Belbel, F. Lalam, Glass. Phys. Chem. 45 (2019) 503–512, https://doi.org/10.1134/S1087659619060087.
[9] M. Harfouche, M. Abdellatief, Y. Momani, A. Abbadi, M. Al Najdawi, M. Al Zoubi, B. Aljamal, S. Matalgah, L.U. Khan, A. Lausi, G. Paolucci, J. Synchrotron Radiat. 29 (2022) 1107–1113, https://doi.org/10.1107/S1600577522005215.
[10] B. Ravel, M. Newville, J. Synchrotron Radiat.12 (2005) 537-541. https://doi: 10.1107/S0909049505012719.
[11] H. Ramdani, Y.I. Bourezg, M. Kharroubi, F. Sahnoune, L. Gacem, Cryst. Res. Technol. 58 (2023) 2200257, https://doi.org/10.1002/crat.202200257.
[12] A. Hamza, M. Kharroubi, J. Non-Cryst. Solid. 560 (2021) 120721, https://doi.org/10.1016/j.jnoncrysol.2021.120721.